JOURNAL OF APPLIED POLYMER SCIENCE VOL. 14, PP. 1449–1471 (1970)

Dynamic Mechanical Properties of Particulate-Filled Composites

T. B. LEWIS and L. E. NIELSEN, *Monsanto Company, St. Louis, Missouri 63166*

Synopsis

The relative shear moduli of composites containing glass spheres in a rubbery matrix obey the Mooney equation, analogous to the relative viscosity of similar suspensions in Newtonian liquids. However, when the matrix is a rigid epoxy, the relative shear moduli are less than what the Mooney equation predicts but greater than what the Kerner equation predicts. Relative moduli are less for rigid matrices than for rubbery matrices because (1) the modulus of the filler is not extremely great compared to that of the rigid matrix; (2) Poisson's ratio is less than 0.5 for a rigid matrix; (3) thermal stresses in the matrix surrounding the particles reduce the apparent modulus of the polymer matrix because of the nonlinear stress–strain behavior of the matrix. This latter effect gives rise to a temperature dependence of the relative modulus below the glass transition temperature of the polymer matrix. Formation of strong aggregates increases the shear modulus the same as viscosity is increased by aggregation. Torsion or flexure tests on specimens made by casting or by molding give incorrect low values of moduli because of a surface layer containing an excess of matrix material; this gives rise to a fictitious increase in apparent modulus as particle size decreases. The mechanical damping can be markedly changed by surface treatment of the filler particles without noticeable changes in the modulus. The Kerner equation, which is a lower bound to the shear modulus, is modified and brought into closer agreement with the experimental data by taking into account the maximum packing fraction of the filler particles.

INTRODUCTION

The discrepancy between theoretical predictions and experimental results for the moduli of particulate-reinforced polymers continues as one of the limitations to the understanding of composite materials. The importance of this arises because particulate systems are often used as a basis for the interpretation of the mechanical behavior of composites in which the filler is of more complex geometry. In addition, a description of the mechanical properties presently requires the use of upper and lower boundaries, which are reviewed in the survey of Hashin.[1]

Here we attempt to resolve several of the differences between theory and experiment by carrying out measurements of the dynamic mechanical properties of a crosslinked polymer reinforced with spherical particles using a torsion pendulum. This system can be accurately defined, several experimental parameters can be varied in a controlled manner, and comparison to theories in the literature can be readily made. The dynamic

properties under investigation include shear modulus G', loss modulus G'', logarithmic decrement or damping Δ, and the glass transition temperature T_g. The experimental variables include particle size and volume fraction of filler, in addition to temperature. The effect on the mechanical properties of silane coupling agents applied to dispersed spheres is presented. Also, experiments are described with the filler being permanent aggregates of spheres characterized by a narrow distribution of number of spheres per aggregate.

The experimental results are used to interpret several equations in the literature. In addition, the results are compared to the recently reported work on the relative viscosity of suspensions of dispersed and permanent aggregates of spheres.

The relation of relative increase in modulus of reinforced solids to relative increase in suspension viscosity was first proposed by Goodier,[2] and Smallwood[3] and Guth[4] showed their equality, i.e.,

$$G_r' = \eta_r \tag{1}$$

with $G_r' = G_c'/G_1'$ and $\eta_r = \eta_c/\eta_1$, where η is viscosity, and r indicates relative value; c, the composite or suspension; and 1, the matrix or suspending fluid. Since this equation was introduced, other papers have also been directed to showing its theoretical validity, but it has been shown experimentally only for limited cases of filled elastomers (see, e.g., Landel and Smith[5]).

A large number of equations of relative modulus of filled systems are in the literature, and they predict a smaller increase with filler concentration[6] than is obtained for shear viscosity of suspensions. One of the more popular of the equations is by Kerner[7] and usually serves as a lower bound. The more recent treatments of the elastic moduli of two-phase and multiphase media use the variational principles of the theory of elasticity.[1]

At the same time, equations have been introduced for shear viscosity which very accurately predict the dependence on filler concentration.[8] The viscosity data have been shown to fit the Mooney equation[9] most accurately, although several equations predict about the same behavior for $\phi_2 \leq 0.20$. To illustrate the difference in predictions of modulus and viscosity, at a filler concentration of $\phi_2 = 0.40$, the viscosity as predicted by Mooney exceeds the modulus value of Kerner by 300%.

Experiments to measure viscosity of suspensions are easier to carry out and can be obtained with a greater degree of accuracy than experiments for modulus. Experimentally, the modulus data generally exhibit a smaller increase than viscosity of suspensions as a function of filler concentration. The usefulness of establishing the extent to which eq. (1) is valid arises because the matrix material of a composite is often initially in the fluid state prior to curing. If relative modulus were equal to, or directly related to, relative viscosity, the value of modulus for the reinforced polymer system in the cured state could be established from a viscosity measurement of a suspension with the uncured polymer.

In the study of relative moduli of filled solids, it is recognized there are three conditions which can affect the modulus value which are not present in suspensions and consequently cannot have any influence on relative viscosity.

The first is the magnitude of the ratio of filler modulus to matrix modulus and the consequent boundary conditions imposed at $\phi_2 = 1.0$ and $\phi_2 = \phi_m$, where ϕ_m is the maximum volumetric packing fraction of filler. At $\phi_2 = 1.0$, the system is entirely filler, so $G_r' = G_2'/G_1'$. The value at ϕ_m is defined as $G_r' = (G_r')^*$, where the magnitude of $(G_r')^*$ is dependent on the value of G_2'/G_1' and ϕ_m. The functional dependence of G_r' and ϕ_2 above and below ϕ_m would be expected to differ since the filler would change from the discontinuous to the continuous phase. However, many equations, including the above-mentioned Kerner expression, are continuous functions for $0 \leq \phi_2 \leq 1.0$. However, it is only meaningful to consider reinforcement in the region $0 < \phi_2 < \phi_m$. In contrast to relative modulus, the following condition holds for relative viscosity:

$$\eta_r \rightarrow \infty \text{ as } \phi_2 \rightarrow \phi_m.$$

The equating of relative modulus to relative viscosity in eq. (1) could only be expected to hold in the limiting case when (G_2'/G_1') is very large and the value of ϕ_m for filled solids equals the value for suspensions. In the common systems of glass–epoxy and boron–epoxy, (G_2'/G_1') is 25 and 125, respectively. Experimentally the maximum volumetric packing fraction[10,11] for a bed of spheres is described as random close packing, with $\phi_m = 0.64$.

The second condition is the presence of induced stresses in the composite. These can arise either from shrinkage of the polymer during cure or owing to the difference in the thermal expansion coefficients of the phases, in which case the stresses develop as the composite cools down after fabrication from the elevated molding temperature or postcure temperature. A recent paper[12] deals with the change in modulus resulting from stresses arising from the mismatch of expansion coefficients and describes the effect on the particular composites under investigation here.

The third condition is the dependence on temperature of two matrix properties: Poisson's ratio and shear modulus. For rigid polymers, Poisson's ratio does not equal 0.5, while above T_g it does equal this value. The magnitude of G_2'/G_1' increases slowly with temperature in the glassy region since the temperature dependences of G_2' and G_1' are not equal, and the ratio increases markedly in the region of T_g.

EXPERIMENTAL

Glass beads in an epoxy matrix are selected for the measurements. The epoxy (Epon 828, Shell Chemical Co.) is diluted with 5% phenyl glycidyl ether (Lot #5HHE112, Shell Chemical Co.) and cured with triethylenetetramine (T-410, Fisher Scientific Co.). The glass beads, soda lime type

(from Microbeads Div. of Cataphote Corp.), are carefully cleaned of the metal particles normally found in this material and are sieved for narrow particle size distributions; the surfaces are cleaned by refluxing in isopropanol. Particle size ranges for the glass spheres are 5–10, 10–20, 30–40, and 75–90 μ. For each of the ranges at least 95% of the particles are within the limits.

The resin is heated in a flask to 40°C and the pressure is reduced to 5 mm Hg to remove absorbed air and water. The beads are added with stirring and dispersed by lowering the flask into an ultrasonic cleaning bath (Sonagen D-50, Branson Instruments, Inc.). The curing agent is added with the suspension at 25°C while stirring. The total suspension is then stirred for about 5 min under vacuum. A sheet of the sample is formed by pouring the filled epoxy suspension between 6 in. × 6 in. glass plates coated with a silane release agent (SC 87, General Electric Co.) and separated by about 0.050 in. The beads are of sufficiently small diameter and the epoxy of a density and viscosity that settling is very slight. The casting is maintained in an exact vertical position for 24 hr at 25°C during which time the initial cure took place. For postcuring, the sample is subjected to an oven cure of 60°C for 3 hr, 100°C for 6 hr, and 140°C for 4 hr after which it is allowed to cool slowly in the oven which had been shut off. The glass transition temperature of the matrix is 121°C. Samples are cut horizontally in the middle section of the castings so that any effect due to settling would be minimized.

An initial cutting of the samples is made with a diamond saw followed by a high-speed router using a carbide tool (Tensilkut, Sieburg Industries, Inc.). The nominal dimensions of the samples are 4 in. × 0.180 in. × 0.050 in.

The dynamic mechanical properties, shear modulus, damping, and glass transition temperature are measured on a recording torsion pendulum.[13] The glass transition is measured as the temperature of the maximum in the mechanical damping peak at about 1 Hz. The theory and discussion of dynamic mechanical testing is presented by Nielsen.[14]

For the experiments with coated glass spheres, silane treatments are applied using the technique described by Kenyon and Duffey.[15] Their tensile strength data on silane-coated glass spheres in epoxy are used as a basis for the selection of the silanes for good and poor adhesion. These are gamma-glycidoxyproplytriethoxysilane (A187, Union Carbide Company) and methylchlorosilanes (SC 87, General Electric Company) for good and poor adhesion, respectively.

The permanent aggregates of spheres used are the identical filler described in the recent paper[16] on viscosity of suspensions with aggregates and contain a specific distribution of particles per aggregate.

Volume fraction of filler is determined by burn-off of resin and density measurements.

Stress–strain results on the pure resin are obtained on samples cast between 6 in. × 6 in. glass plates with a separation of $^1/_8$ in. and machined

as standard ASTM D-638 samples. The measurements are carried out with an Instron testing machine (Instron, Canton, Mass.) at a strain rate of 0.01 min^{-1}.

RESULTS AND TREATMENT OF DATA

Shear modulus and damping for the dispersed spheres in the epoxy matrix are measured as a function of temperature for several values of volume fraction and particle size of filler. The temperature range normally is from 100°C below to 50°C above the glass transition temperature. The amount of filler in the samples varies from unfilled to a volume fraction of about 0.40.

Representative data are shown in Figure 1 for shear modulus G', logarithmic decrement or damping Δ, and calculated loss modulus G'' versus temperature for samples of pure matrix and a high volume fraction of spheres. (G'' is determined using experimental values of G' and Δ in the expression $G'' = \Delta G'/\pi$.) The reproducibility of measuring shear moduli is 2%–3%, and for damping it is ±5%. Although most of the results in this paper are in the temperature range 100°C below to 50°C above the glass transition, the data in Figure 1 include results at lower temperatures extending to the region of a secondary glass transition. The behavior illustrated with these curves indicates that in general when a filled system is compared to an unfilled material, the values of the moduli G' and G'' show an increase and damping Δ decreases. Here, the transition between the glass and rubbery regions is specified as T_g and defined by the maximum in the damping curve.

For shear modulus below the glass transition, log G' decreases linearly with T and about 20°C below T_g starts the decrease of nearly two orders of magnitude and levels off about 10°C above T_g. The negative slope in the linear region of the log G'–T curve below the glass transition is a function of volume fraction filler and accounts for the positive slope of the relative modulus–temperature curves in Figure 2. The change in relative modulus with temperature is primarily due to induced tensile stresses by the difference in thermal expansion coefficients of the phases.[12] If the stresses were not present, the value of relative modulus at all temperatures would be the value obtained by extrapolation of the data points below T_g in Figure 2 to the glass transition where the stresses are zero. The shape of the shear modulus curves above T_g changes with volume fraction filler, as is shown in Figure 1. Although this is also exhibited in similar systems in the literature, there is no apparent explanation. A positive slope for log G'–T is predicted by the kinetic theory of rubber-like elasticity. In the presence of filler, the positive slope is not observed and G' remains constant with the temperature, except for the cases of $\phi_2 \geq 0.40$, and then G' shows a small decrease with temperature.

The change in the glass transition with the incorporation of filler in a polymer is treated extensively in the literature (see, e.g., Landel,[17] Kumins

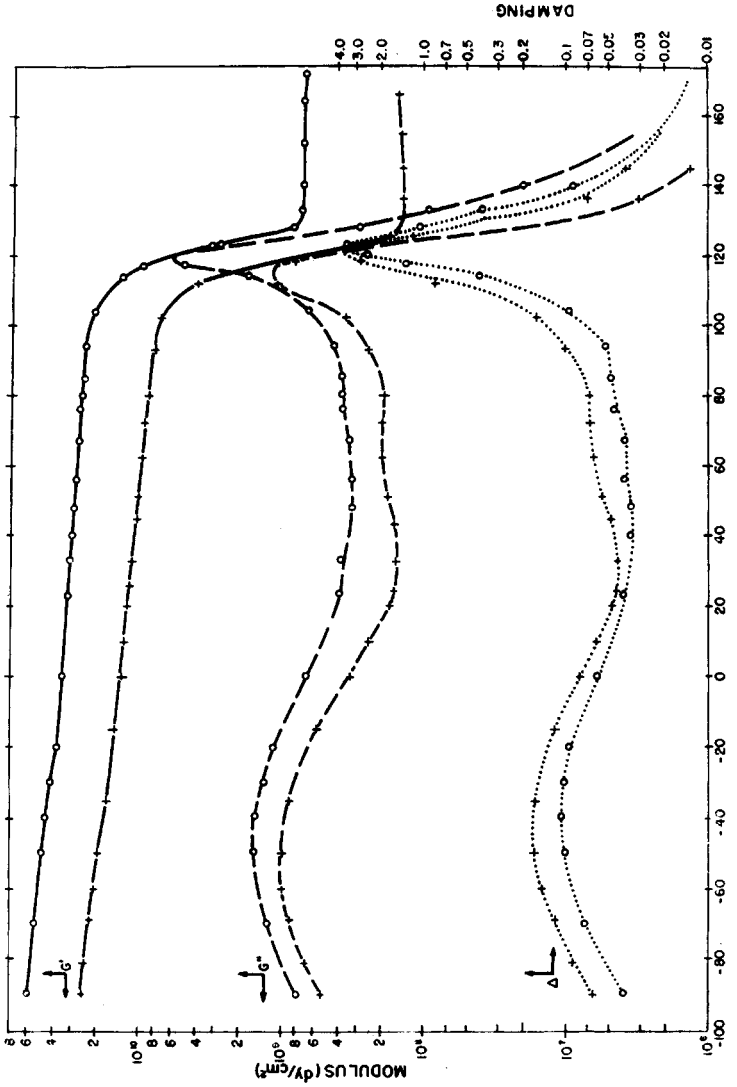

Fig. 1. Shear modulus (—), loss modulus (– –), and damping (····) vs. temperature for unfilled epoxy (+) and epoxy with 0.41 volume fraction (○) spheres of diameter 10–20 μ.

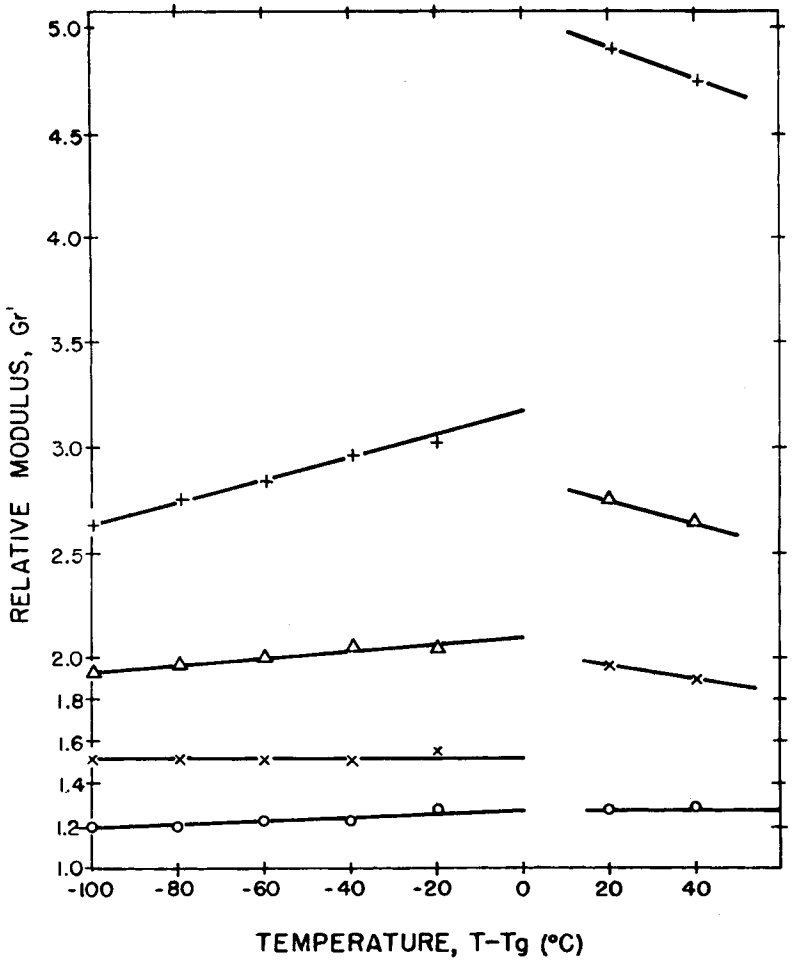

Fig. 2. Relative modulus vs. temperature for epoxy with spheres of diameter 10–20 μ. Solid curves are drawn through the experimental points to indicate the modulus–temperature slopes: (+) $\phi_2 = 0.41$; (Δ) $\phi_2 = 0.30$; ($\times$) $\phi_2 = 0.19$; (O) $\phi_2 = 0.10$.

and Roteman,[18] Lipatov et al.,[19] Shreiner et al.,[20] and Smit[21]). Here, only a quite small increase in T_g is observed, as indicated in Table I for various conditions of particle size and volume fraction.

The accuracy associated with damping measurements is valid for values of $\Delta \leq 1.0$, above which the accuracy is greatly reduced due to difficulty in making the measurement. Smooth curves are drawn through all of the sets of experimental damping data with a maximum of $\Delta_m = 3.0$; however, there is no significance to be attached to a fixed value of Δ_m for all experimental conditions, except that it is a typical value.

For the few experiments in the region of the low-temperature secondary glass transition, the damping curve is very broad and the modulus curve

TABLE I
Glass Transition and Relative Modulus Data

Diameter, μ	ϕ_2	T_g	G_r' at $(T - T_g)$				
			−100°C	−80°C	−60°C	−40°C	−20°C
5–10	0.26	122	1.85	1.88	1.93	1.98	1.99
10–20	0.10	122	1.20	1.19	1.22	1.22	1.28
	0.19	123	1.52	1.51	1.51	1.51	1.57
	0.30	123	1.93	1.97	2.00	2.06	2.04
	0.41	123	2.63	2.75	2.84	2.97	3.03
30–40	0.10	123	1.18	1.19	1.20	1.22	1.23
	0.23	123	1.56	1.57	1.58	1.61	1.62
	0.30	123	1.89	1.97	2.04	2.08	1.96
	0.40	124	2.41	2.50	2.60	2.64	2.49
75–90	0.02	121	1.03	1.03	1.02	1.0	1.0
	0.05	121	1.10	1.12	1.10	1.10	1.10
	0.10	121	1.23	1.21	1.20	1.17	1.19
	0.15	122	1.27	1.29	1.29	1.29	1.30
	0.19	122	1.49	1.49	1.46	1.46	1.49
	0.24	122	1.66	1.66	1.64	1.64	1.66
	0.31	122	1.94	1.91	1.91	1.91	1.91
	0.32	122	1.94	1.95	1.96	1.98	1.96
	0.38	123	2.32	2.34	2.38	2.44	2.41

shows very little deviation with temperature from one side to the other of the transition, as indicated in Figure 1.

Relative Modulus of Dispersed Spheres

The reinforcement in shear modulus produced by filler concentration in a particulate reinforced polymer sample is normally described relative to the value of the unfilled sample and is computed for a given volume fraction at temperatures relative to the glass transition, i.e., at $T - T_g$, for the unfilled and filled samples. In Figure 2, typical data of relative modulus are plotted at four volume fractions for spheres of diameter d = 10–20 μ. Because of the very large changes in absolute values of modulus at temperatures in the transition region, it is not meaningful to include points for temperatures near T_g. Marked differences in G_r' can be observed for temperatures above and below T_g. There is more than a 50% increase in relative modulus from below to above T_g for samples with $\phi_2 > 0.30$. This is in general agreement with experimental results considered by Nielsen.[14] Below T_g, a dependence on temperature for G_r' is indicated by the positive slope for each modulus–temperature curve. Similar behavior to that shown in Figure 2 is observed for all particle sizes, although the slopes are not as large with increased particle diameter.

In Table I, values of G_r' are included for the different particle size ranges at several temperatures and volume fractions.

For comparison to theory, relative moduli are usually plotted versus volume fraction, and typical data are shown in Figure 3 below the glass

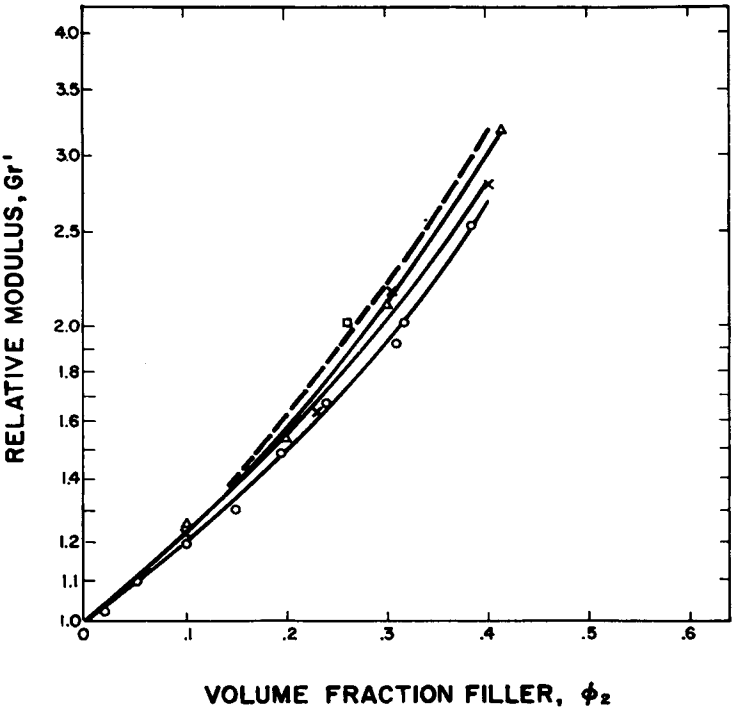

Fig. 3. Relative modulus vs. volume fraction filler for dispersed spheres in epoxy. Solid curves are drawn through d = 10–20 μ, 30–40 μ, and 75–90 μ data points. Data points correspond to a temperature extrapolation in the region below the glass transition to $T = T_g$. Dashed curve is obtained by extrapolation of results to $d = 0$: (□) d = 5–10 μ; (△) d = 10–20 μ; (×) d = 30–40μ: (○) d = 75–90μ.

transition for different particle size ranges. In order to eliminate the effect of induced stresses on modulus, the data for Figure 3 are obtained by extrapolation of relative modulus–temperature data to T_g. In Figure 4, relative modulus-versus-volume fraction curves are plotted for particle size ranges above T_g. In this case, the temperature is T_g + 20°C.

In addition to the dependence of relative modulus on temperature, there is an increase in relative modulus with decreasing particle size, as indicated in Figures 3 and 4.

For the relative viscosity measurements, no particle size effect for the size range of interest is observed, in contrast to the one observed for relative modulus. Here, the change with filler diameter is either a characteristic of these systems or due to an instrumental error. A consideration of the shear field produced within the sample during the torsional oscillation suggests the validity of the latter reason. The shear stress is a maximum at the outer edges and faces and zero at the center.[22] In the direction of the thickness t of the sample, the stress can be assumed to rise linearly from zero to the maximum stress level at the two faces of the sample. It is in the region of the faces that there is the poorest distribution of the filler and a

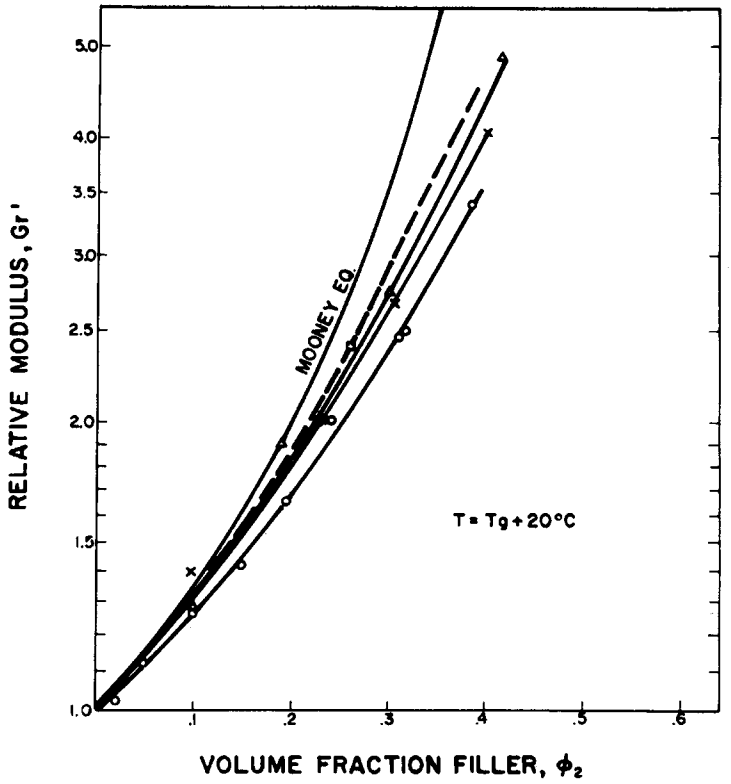

Fig. 4. Relative modulus vs. volume fraction for dispersed spheres in epoxy above the glass transition at $T = T_g + 20°C$. Solid curves are drawn through the d = 10–20 μ, 30–40 μ, and 75–90 μ data points. Dashed curve is obtained by extrapolation of the results to $d = 0$. A plot of the Mooney equation is also included: (□) d = 5–10 μ; (△) d = 10–20 μ; (×) d = 30–40 μ; (○) d = 75–90 μ.

larger portion of matrix, i.e., greater than $(1 - \phi_2)$, since the samples were cured between two flat surfaces. The larger spheres lead to a worse condition since there is a larger absolute distance over which the resin is present in excess. Also, in the center region of the sample, the filler must be present in excess for a specific value of ϕ_2, and thus the extent of nonuniformity in distribution increases with particle size. The effect of particle diameter is minimized only in the limit as (d/t) approaches zero.

In order to account for any effect due to the shear field and the corresponding contribution to G_r' of excess resin at the sample faces, the data are extrapolated to $d = 0$ in Figure 5. The points for Figure 5 are taken from the solid curves in Figures 3 and 4 at $\phi_2 = 0.26$, and the experimental data for d = 5–10 μ, at $\phi_2 = 0.26$. The extrapolated values are 2.44 for $T = T_g + 20°C$ and 1.96 for $T < T_g$. Curves for an extrapolation to $d = 0$ are included in Figures 3 and 4. They are obtained by assuming that the slopes of the two solid lines in Figure 5 are equal to the product of a con-

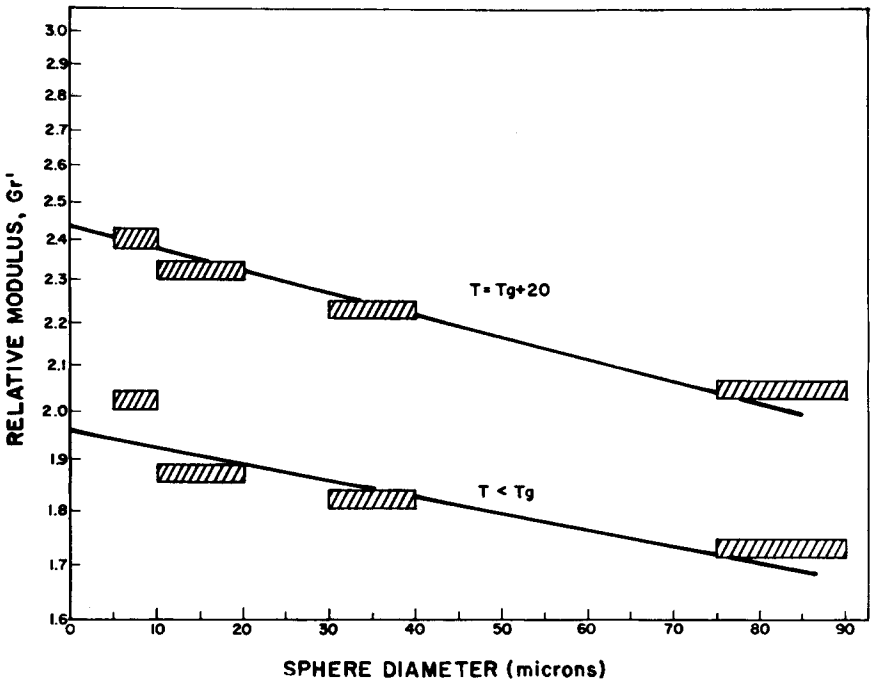

Fig. 5. Plot of log relative modulus vs. particle size range at a volume fraction filler of 0.26. Data are obtained from solid curves in Figures 3 and 4 for d = 10–20 μ, 30–40 μ, and 75–90 μ, in addition to the d = 5–10 μ experimental data. Data are plotted with a $\pm$ 1% error bracket.

stant and the volume fraction. The extrapolated values at other volume fractions are obtained using this constant, the respective ϕ_2 values, and data from Figures 3 and 4.

Damping and Loss Modulus

The data shown in Figure 1 for damping Δ and loss modulus G'' indicate the general behavior when particulate filler is added to polymer. All of the curves with dispersed spheres are very similar in shape. One measure of damping is the width of the peak, i.e., the temperature interval for which damping exceeds 0.5. This interval is 18°C for all conditions of volume fraction and sphere diameter.

The glass transition temperature increases only slightly with volume fraction and is the source of a slight shift of the curves with volume fraction.

If the damping in a filled polymer results only from the same mechanisms which produce the damping in the unfilled matrix, then the following ratio holds[23]:

$$\frac{\Delta F}{\Delta_{10}} = \phi_1 \tag{2}$$

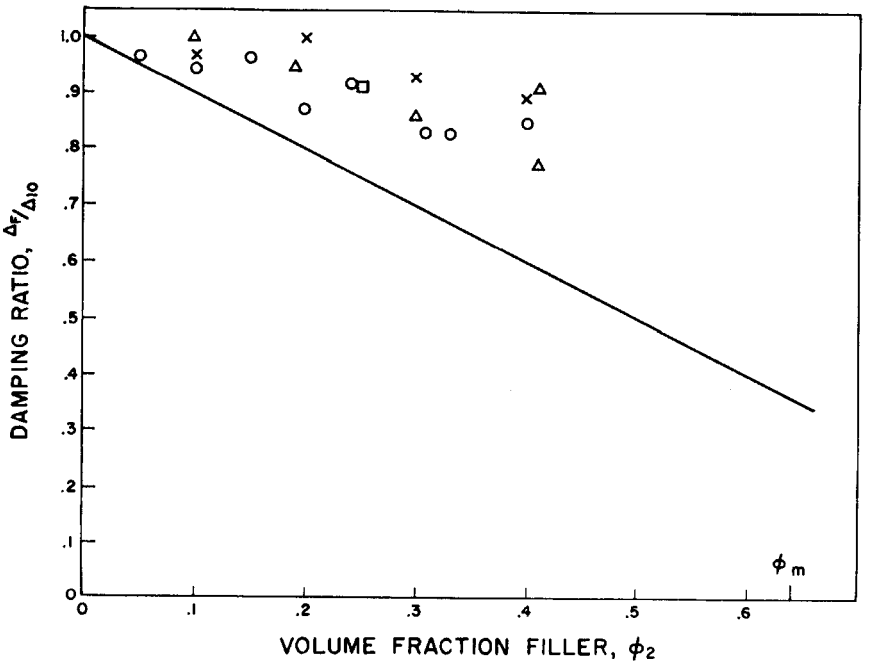

Fig. 6. Ratio of damping of filled polymer to unfilled matrix, Δ_F/Δ_{10}, vs. volume fraction filler at a temperature of 100°C below T_g. The solid curve is a plot of $\Delta_F/\Delta_{10} = (1 - \phi_2) = \phi_1$: (□) d = 5–10 μ; (△) d = 10–20 μ; (×) d = 30–40 μ; (○) d = 75–90 μ.

where Δ_{10} indicates damping of the unfilled matrix and Δ_F is the damping at matrix volume fraction ϕ_1. The ratio Δ_F/Δ_{10} is plotted for T = 25°C in Figure 6 for all of the glass sphere–epoxy experiments, and a solid curve indicates eq. (2). All of the experimental points are above the solid line, indicating additional damping mechanisms are present at all volume fractions. The damping data are listed in Table II.

Damping in addition to the prediction of eq. (2) is expected from three sources. If the particle size effect on modulus is due to the instrumental effect described above, additional damping arises from the excess resin at the faces of the sample. The thermal stresses arising from the mismatch in thermal expansion coefficients of the phases produce a decrease in relative modulus and an increase in damping in the room temperature range. Also, there is an anomalous small increase in damping which starts at 60°C, but which could have an effect at room temperature. This anomalous increase occurs under certain conditions which cannot be correlated with any of the experimental parameters. When the rise is not present, damping increases gradually from 25°C to the start of the transition region. When the increase is present, it is small, from about 0.04 to 0.06, and occurs at about 60°C. The damping then levels off to the start of the transition. One possible explanation is that this damping results from friction at the inter-

TABLE II
Damping Data

Diameter	ϕ_2	Δ at $(T - T_g)$ −100°C	−80°C	−60°C	−40°C	−20°C
		Dispersed Spheres (Untreated)				
Δ_{10}[a]	0	.043	.046	.065	.070	.145
Δ_{10}[b]	0	.045	.047	.054	.064	.116
Δ_{10}[c]	0	.047	.047	.051	.063	.120
5–10 μ	0.26	.039	.040	.046	.056	.120
10–20 μ	0.10	.043	.046	.058	.067	.120
	0.19	.045	.050	.062	.073	.150
	0.30	.037	.041	.053	.065	.132
	0.41	.039	.037	.038	.046	.084
30–40 μ	0.10	.046	.042	.050	.056	.105
	0.23	.045	.044	.044	.054	.099
	0.30	.042	.042	.042	.052	.110
	0.40	.039	.039	.040	.047	.108
75–90 μ	0.02	.041	.045	.064	.072	.140
	0.05	.045	.047	.051	.059	.105
	0.10	.044	.045	.060	.071	.135
	0.15	.045	.045	.052	.062	.120
	0.19	.041	.047	.053	.062	.108
	0.24	.043	.045	.056	.060	.125
	0.31	.039	.042	.050	.062	.110
	0.32	.039	.043	.049	.059	.110
	0.38	.040	.040	.042	.051	.110
		Dispersed Spheres (Treated)				
75–90 μ						
A187	0.30	.041	.036	.040	.052	.110
SC 87	0.30	.049	.048	.048	.054	.119
SC 87 (thick)	0.30	.068	.072	.074	.081	.125
		Aggregated Spheres (15–22 Spheres per Unit)				
	0.05	.046	.050	.056	.069	.125
	0.19	.040	.043	.046	.058	.118

[a] Unfilled results for matrix used with spheres of d = 5–10 μ and 10–20 μ, and aggregates.

[b] Unfilled results for matrix used with spheres of d = 30–40 μ and treated spheres.

[c] Unfilled results for matrix used with spheres of d = 75–90 μ.

face between matrix and filler and occurs irregularly due to some difference in the fabrication procedure of the specimens in which it is observed.

The effect on damping of surface treatments applied to the filler surface is observed by comparison to damping of samples with untreated dispersed spheres. For the purpose of comparison, all conditions except the type of silane are the same. The silanes for good and poor adhesion are A187 and SC 87, respectively (see experimental section). With SC 87, the spheres could only be dispersed if the silane is applied from a very dilute solution

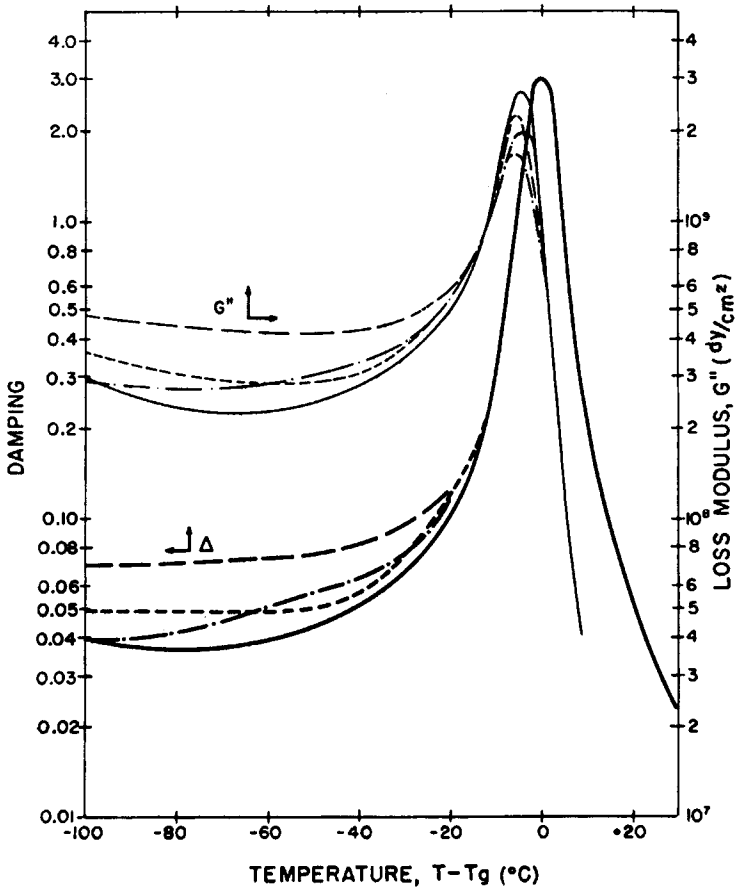

Fig. 7. Damping and loss modulus vs. temperature for epoxy filled with 0.30 volume fraction spheres treated with silanes and untreated: (—) A187, (– – –) SC 87; (– –) SC 87 (thick); (-·-·-) untreated.

(≪1% in carbon tetrachloride). With a solution of 0.5% SC 87 in carbon tetrachloride, the thicker coating produces noticeable agglomeration.

The shear moduli curves for treated and untreated spheres are essentially identical. Clear differences are evident with damping and loss modulus, as shown in Figure 7. The glass transition temperatures are listed in Table III and show a decrease with A187 and an increase with SC 87.

TABLE III
Glass Transition Temperatures

Treatment	ϕ_2	T_g, °C
A187	0.30	122
none	0.31	122
SC 87	0.30	125
SC 87 (thick)	0.30	126

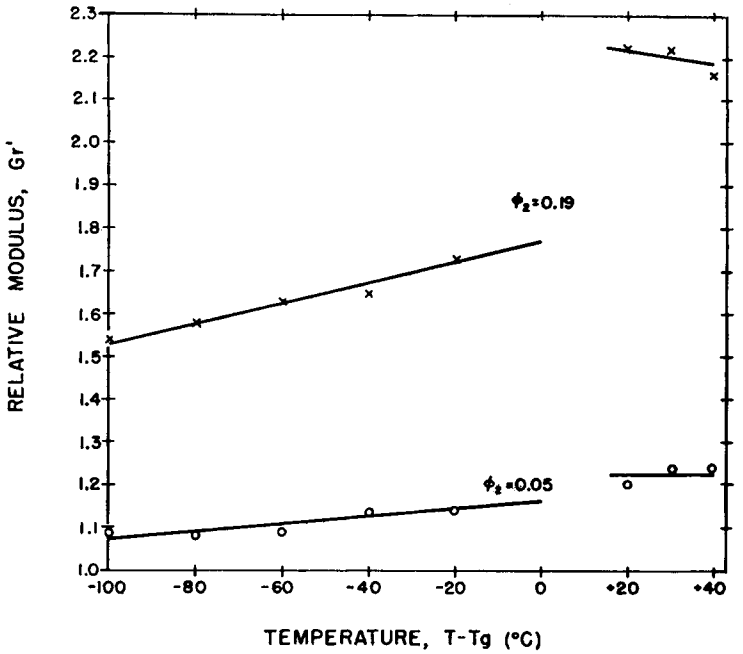

Fig. 8. Relative modulus vs. temperature for aggregated spheres in epoxy at two volume fractions. For comparison to data with dispersed spheres, the extrapolated values of relative modulus from Figures 3 and 4 are: $(T < T_g)G_r' = 1.57$ for $\phi_2 = 0.19$, $G_r' = 1.11$ for $\phi_2 = 0.05$; $(T = T_g + 20°C)$ $G_r' = 1.81$ for $\phi_2 = 0.19$; $G_r' = 1.14$ for $\phi_2 = 0.05$.

Below T_g the magnitudes of Δ and G'' are less with A187 coatings compared to untreated and SC 87-treated spheres; the SC 87-treated spheres produce larger damping and loss moduli. The peak in the G'' curve is narrower with SC 87-treated filler and the shape of the curves reflect the shift in T_g. The shape of the Δ curves indicates that for spheres coated with A187 and untreated there is a gradual increase with temperature from room temperature to temperatures just below the beginning of the large rise in damping due to the polymer's main transition. In the two cases with SC 87 coatings, the damping curves are flat from room temperature until temperatures at the start of the main transition. The width of the peaks remain nearly the same for all of the conditions. Above the glass transition, it is not possible to distinguish damping and loss modulus for composites with treated and untreated filler.

Moduli of Aggregates

The relative modulus of permanent aggregates of spheres incorporated into the epoxy resin is shown in Figure 8 for two volume fractions, $\phi_2 = 0.05$ and $\phi_2 = 0.19$. This is the first time dynamic measurements are reported on a polymer filled with aggregates characterized according to size,

shape, and number of spheres per aggregate. These are the same aggregates as used in the experimental determination of viscosity of suspensions with aggregated spheres.[16] Although the viscosity measurements are reported for a series of narrow size ranges, these experiments are limited to one of the size ranges. A size range of 15–22 spheres per aggregate is selected for two reasons: according to viscosity results these aggregates are large enough for behavior of aggregates to be clearly distinguishable from spheres; the instrumental error due to absolute size of particles, discussed above, is kept to a minimum.

The significant result is that the relative moduli in the range $T < T_g$ exceed the extrapolated curves to zero diameter for dispersed spheres (Fig. 3), while the average diameter of the aggregates is 130 μ. In the temperature range $T > T_g$, the relative moduli exceed the Mooney curve and the extrapolated $d = 0$ curve.

Because of the size of the aggregates, the modulus values for these two volume fractions could not be expected to approach the values of relative viscosity obtained in the measurements with suspensions. The values of η_r with the aggregates are 6.0 and 1.27 for volume fractions of $\phi_2 = 0.19$ and $\phi_2 = 0.05$, respectively. The maximum values of G_r at $T > T_g$ for the same values of ϕ_2 are 2.25 and 1.25, respectively.

Damping as measured by log decrement Δ or G''/G' is considerably reduced compared to damping of dispersed spheres at the same volume fractions. Listed in Table II are the values of Δ_c and Δ_c/Δ_{10}, where Δ_c and Δ_{10} represent damping with the composite and unfilled polymer, respectively.

Tensile Properties of the Matrix

The stress–strain properties of the unfilled epoxy resin are shown in Figure 9 for three temperatures below T_g. The tensile experiments of the unfilled polymer are of interest because the relative moduli of the composites are defined relative to the unfilled polymer. We recently attributed the temperature dependence of relative modulus of reinforced polymers to the mismatch of the thermal expansion coefficients of the phases and the resulting tensile stresses in the matrix. Because of the stresses, the modulus of the polymer in the vicinity of each filler particle is lower than the modulus of unfilled polymer E_{10}, even though the modulus of the filled system E_c is greater than that of unfilled polymer.

The tensile properties of the resin are used to describe the extent to which the matrix modulus changes, which is used to predict the temperature dependence of the relative modulus of the filled polymer.

Since stress σ is a nonlinear function of strain ϵ for polymers, it can be expressed as[12]

$$\sigma = a\epsilon + b\epsilon^2 + \ldots \tag{3}$$

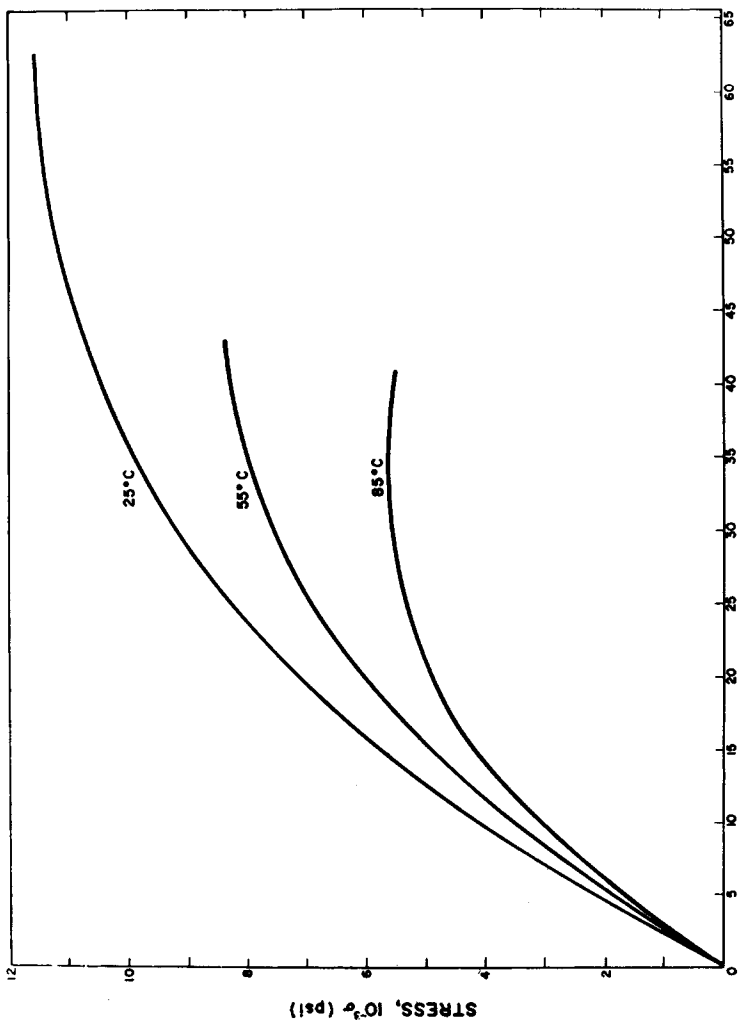

Fig. 9. Tensile stress vs. strain for the unfilled epoxy at three temperatures.

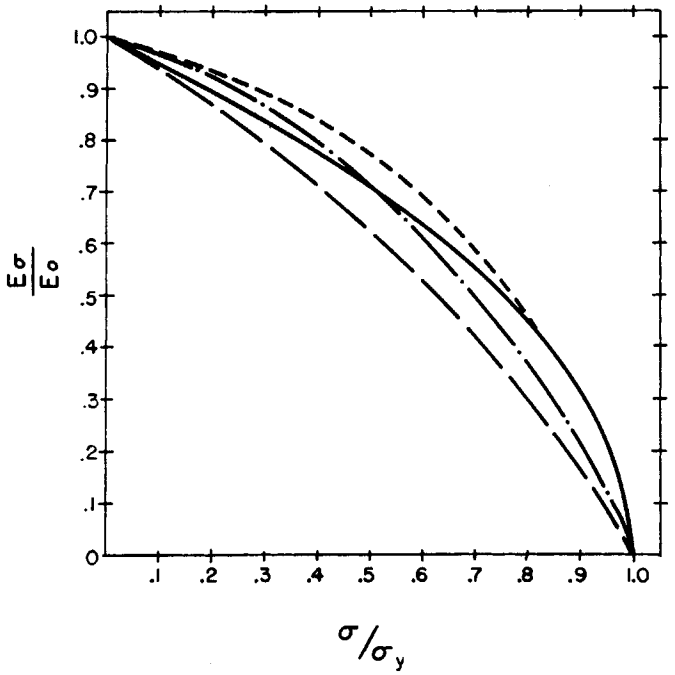

Fig. 10. Radio of tangent modulus to Young's modulus of matrix, $E\sigma/E_0$, vs. ratio of stress to yield stress, σ/σ_y, at three temperatures. A plot of eq. (4) is also included: (—) eq. (4); (– –) 25°C; (–·–) 55°C; (—) 85°C.

The boundary conditions lead to the following expression for the slope of the stress–strain curve E_σ at stress level σ:

$$E_\sigma = E_{10}\left(1 - \frac{\sigma}{\sigma_y}\right)^{1/2} \tag{4}$$

where E_{10} is Young's modulus of the matrix and σ_y is the yield stress of the matrix defined by an extrapolation of the curves in Figure 9 to zero slope. Values of (E_σ/E_{10}), calculated from the stress–strain data for the three temperatures, are shown in Figure 10 along with a curve corresponding to $[1 - (\sigma/\sigma_y)]^{1/2}$. The fairly close agreement between experiment and the value of $[1 - (\sigma/\sigma_y)]^{1/2}$ indicates the series expansion is a good representation of the stress–strain behavior. Also, the curves indicate the amount that the tangent modulus of a material can be decreased owing to residual stresses.

MODIFICATION OF KERNER EQUATION

Agreement between the relative modulus and relative viscosity is expected only for the case of $G_2'/G_1' \to \infty$. For all finite values, the boundary conditions at $\phi_2 = 1.0$ and $\phi_2 = \phi_m$ depress the volume fraction dependence of G_r' over the range of $0 < \phi_2 < \phi_m$. However, the effect of G_2'/G_1' is to lower the relative modulus to a greater extent below T_g compared to above T_g.

The Mooney equation,

$$\ln \eta/\eta_1 = \frac{k_E\phi_2}{1 - (\phi_2/\phi_m)}, \tag{5}$$

which characterizes the dependence of relative viscosity on volume fraction for a suspension of dispersed spheres, should also hold for shear moduli, provided Poisson's ratio of the matrix is 0.5 and G_2'/G_1' is a very large number. In this equation k_E is the Einstein coefficient, equal to 2.5 for dispersed spheres. Because of the above restrictions, the Mooney equation is not adequate when the matrix is a rigid material. For rigid matrices, the Kerner equation[7] or the analogous Hashin-Shtrikman equation[24] is the best approximation to the experimental values, although these equations are lower bounds and predict values less than the experimental values.

The Kerner equation may be put in the form[25]

$$\frac{G_c'}{G_1'} = \frac{1 + AB\phi_2}{1 - B\phi_2} \tag{6}$$

where

$$A = \frac{7 - 5\nu_1}{8 - 10\nu_1} \text{ and } B = \frac{(G_2'/G_1') - 1}{(G_2'/G_1') + A}. \tag{7}$$

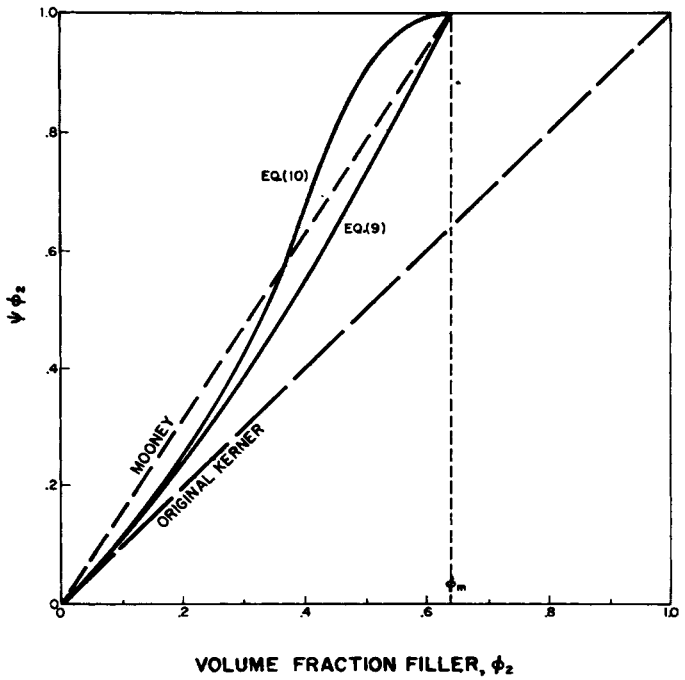

Fig. 11. Plot of eqs. (9) and (10) for a packing volume of 0.64 compared with the analogous behavior for the Mooney and original Kerner equations.

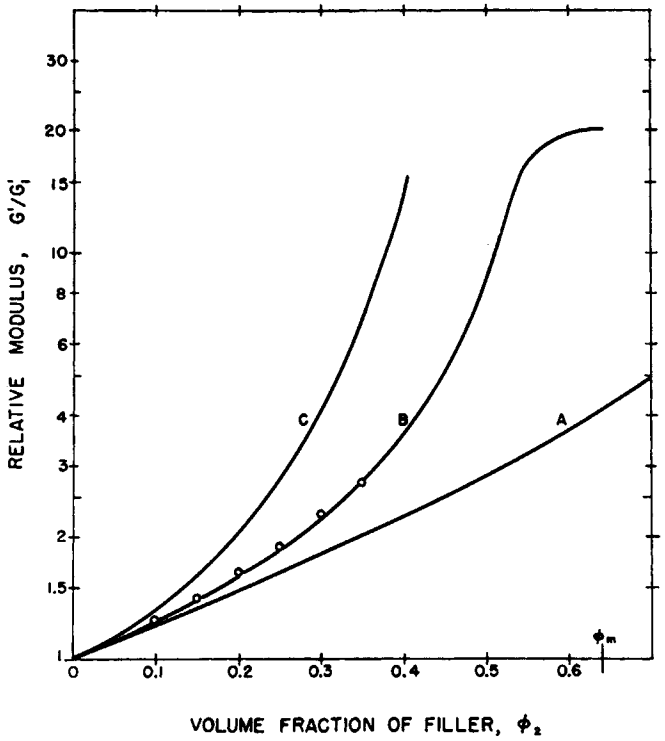

Fig. 12. Dependence of relative modulus on concentration for (A) the original Kerner equation; (B) the modified Kerner equation; (C) the Mooney equation. Circles correspond to experimental results as plotted in Figure 3. Solid curves are calculated with $\nu_{12} = 0.35$, $G_2/G_{11} = 25$, and $\phi_m = 0.64$.

Improvement can be made by taking into account the maximum packing fraction ϕ_m by the introduction of an additional function ψ to modify the Kerner equation in a manner analogous to the Mooney equation, as follows:

$$\frac{G_c'}{G_1'} = \frac{1 + AB\,\phi_2}{1 - B\psi\phi_2}. \tag{8}$$

The boundary conditions imposed upon $\psi\phi_2$, are:

(1) $\psi\phi_2 = 0$ at $\phi_2 = 0$;

(2) $\dfrac{d(\psi\phi_2)}{d\phi_2} = 1$ at $\phi_2 = 0$;

(3) $\psi\phi_2 \doteq 1$ at $\phi_2 = \phi_m$.

The first two of these conditions ensure Einstein behavior at low concen-

trations. Two of the simplest functions that fulfill these conditions and which give reasonable agreement with experimental results are:

$$\psi\phi_2 = \left[1 + \left(\frac{1 - \phi_m}{\phi_m^2}\right)\phi_2\right]\phi_2; \tag{9}$$

$$\psi\phi_2 = 1 - \exp\left(\frac{-\phi_2}{1 - (\phi_2/\phi_m)}\right). \tag{10}$$

These equations are illustrated in Figure 11.

Figure 12 compares the experimental data on the epoxy resin filled with glass beads, the original Kerner equation, the generalized Kerner equation using $\phi_m = 0.64$ and eq. (10) for $\psi\phi_2$, and the Mooney equation. The theoretical Kerner equations are still both lower bounds, but the introduction of ϕ_m brings the predicted values much closer to the experimental values.

DISCUSSION OF EXPERIMENTAL RESULTS

The data presented here for shear modulus and damping of the epoxy–glass composites and also for the tensile properties of the matrix are sufficient for a complete description of the dynamic properties of particulate reinforced polymers.

The relative shear moduli for dispersed and aggregated particles are clearly different as indicated in Figures 2 and 8. The volume fraction dependence can be described very accurately for dispersed spheres as shown in Figures 3 and 4. The dependence of G_r' on ϕ_2 is very dependent on G_2'/G_1' and very probably on ϕ_m also, as described in the previous section. The data below and above T_g correspond to values of G_2'/G_1' equal to 25 and 2000, respectively. It was not possible to vary ϕ_m with dispersed spheres, but the aggregated spheres represent a filler with ϕ_m much less than the value for dispersed spheres.

The contributions to the relative shear modulus from both the particle size effect and the induced tensile stresses are evaluated by extrapolations. The amount of the contribution because of increasing particle diameter is estimated by an extrapolation of sphere diameter, whereas for the induced stresses, the data below the glass transition are extrapolated as a function of temperature to T_g, where the magnitude of the induced stresses is zero. The experimental data taking into account both extrapolations are shown in Figure 12.

These effects of induced stresses and filler particle size are not essential to a general description of the relative modulus behavior of a reinforced polymer. The data here include both effects and the magnitude of each is approximated by the extrapolation. The contributions from these effects are very likely the reason for the discrepancies between different sets of experimental data in the literature, and also between experimental and theoretical results.

An interpretation of the dynamic properties requires that effects associated with damping are also related to relative modulus results. Thus,

the additional damping mechanisms producing the condition $(\Delta F/\Delta_{10}) > \phi_1$ are a factor in determining the relative shear modulus behavior. For this reason, identification of contributions to relative modulus from particle size and induced stress effects is evidence they are sources of additional damping in the system.

The condition of a surface treatment such as SC 87 increasing the damping of a filled system to a level higher than the unfilled resin indicates the usefulness of such particulate-reinforced materials for increased damping compared to the unfilled material.

Low damping is obtained with samples reinforced with aggregates of spheres, and this is an indication that the matrix can be divided into "free" and "entrapped" portions, as in the case of the fluid for the relative viscosity measurements on suspensions of aggregates.

The damping is produced by the volume fraction of resin which is free, while the entrapped matrix essentially reduces the value of ϕ_m, indicating the relative modulus increases with volume fraction at a faster rate for aggregates compared to dispersed spheres.

Our recent paper on the temperature dependence of relative modulus below T_g describes the decrease in G_r' with decreasing temperature as the result of induced tensile stresses in the matrix of the composite. For polymeric matrices, the tensile properties of the resin are important since they establish the extent to which the stiffness and strength of the composite are decreased. Generally, it is very difficult to use the induced stresses to advantage, because if they improve the reinforcement in one direction, a decrease in properties in the plane perpendicular to this direction is expected. The requirement to closely match the thermal expansion coefficients of the constituents follows directly. For the epoxy and glass sphere data for $\phi_2 = 0.41$ in Figure 2, almost 20% of the increase in modulus obtained with the filler is lost at room temperature primarily because of the induced stresses.

Schwarzl et al.[26,27] have shown that the theory of van der Poel[28] seems to hold for the moduli of filled polymers. There are two assumptions in van der Poel's development which do not seem to be consistent with the experimental data. The theory assumes that Poisson's ratio for the matrix is always 0.5 and, also, it does not take into account the maximum allowable packing of the reinforcing phase ϕ_m. For these reasons we believe the modified Kerner equation represents the available data better than does the theory of van der Poel.

The authors wish to thank Mr. David M. Hemmerly who carried out most of the experimental work, Dr. A. S. Kenyon for several helpful discussions, and Mr. H. E. Carter and Miss Anne Gordon for their assistance during various parts of this research.

Contribution HPC 69-88 from the Monsanto/Washington University Association sponsored by the Advanced Research Projects Agency, Department of Defense, under Office of Naval Research Contract N00014-67-C-0218, ARPA Order No. 876.

References

1. Z. Hashin, *Appl. Mech. Rev.*, **17**, 1 (1964).
2. J. N. Goodier, *Phil. Mag.*, **22**, 678 (1936).
3. H. M. Smallwood, *J. Appl. Phys.*, **15**, 758 (1944).
4. E. Guth, *J. Appl. Phys.*, **16**, 20 (1945).
5. R. F. Landel and T. Smith, *ARS J.*, **31**, 599 (1961).
6. L. E. Nielsen, *J. Composite Materials*, **2**, 120 (1968).
7. E. H. Kerner, *Proc. Phys. Soc. (B)*, **69**, 808 (1956).
8. I. R. Rutgers, *Rheol. Acta*, **2**, 202, 305 (1962).
9. M. Mooney, *J. Colloid Sci.*, **6**, 162 (1951).
10. G. D. Scott, *Nature*, **188**, 908 (1960).
11. R. K. McGeary, *J. Amer. Ceram. Soc.*, **44**, 513 (1961).
12. L. E. Nielsen and T. B. Lewis, *J. Polym. Sci. A-2*, **7**, 1705 (1969).
13. L. E. Nielsen, *Rev. Sci. Instr.*, **22**, 960 (1951).
14. L. E. Nielsen, *Mechanical Properties of Polymers*, Reinhold, New York, 1962, pp. 138–201.
15. A. S. Kenyon and H. J. Duffey, *Polym. Eng. Sci.*, **7**, 189 (1967).
16. T. B. Lewis and L. E. Nielsen, *Trans. Soc. Rheol.*, **12**, 421 (1968).
17. R. F. Landel, *Trans. Soc. Rheol.*, **2**, 53 (1958).
18. C. A. Kumins and J. Roteman, *J. Polym. Sci. A*, **1**, 527 (1963).
19. Y. S. Lipatov, T. E. Lipatova, Y. P. Vasilienko, and L. M. Sergeyeva, *Polym. Sci. USSR*, **4**, 920 (1963).
20. S. A. Shreiner, P. I. Zubov, T. A. Volkova, and I. I. Vokulovskaya, *Colloid J. USSR*, **26**, 541 (1965).
21. P. P. A. Smit, *Rheol. Acta*, **5**, 277 (1966).
22. S. Timoshenko and J. N. Goodier, *Theory of Elasticity*, McGraw-Hill, New York, 1951, pp. 258–315.
23. L. E. Nielsen, *Trans. Soc. Rheol.*, **13**, 141 (1969).
24. Z. Hashin and S. Shtrikman, *J. Mech. Phys. Solids*, **11**, 127 (1963).
25. S. W. Tsai, *Formulas for the Elastic Properties of Fiber-Reinforced Composites*, AD 834851 (June 1958).
26. F. R. Schwarzl, H. W. Bree, and C. J. Nederveen, in *Proceedings of 4th International Congress of Rheology*, 1963, E. H. Lee, Ed., Interscience, New York, 1965, Pt. 3, pp. 241–263.
27. F. R. Schwarzl, H. W. Bree, C. J. Nederveen, G. A. Schwippert, L. C. E. Struik, and C. W. van der Wal, *Rheol. Acta*, **5**, 270 (1966).
28. C. van der Poel, *Rheol. Acta*, **1**, 198 (1958).

Received March 6, 1970